forests

MDPI

Article

Assessing the Versatility of Bioextraction to Preserve Waterlogged Wood

Mathilde Monachon [1], Charlène Pelé-Meziani [2], Sathiyanarayanan Ganesan [1], Sabine de Weck [3], Friederike Moll-Dau [4], Janet Schramm [5], Katharina Schmidt-Ott [5] and Edith Joseph [1,3,*]

[1] Laboratory of Technologies for Heritage Materials, Institute of Chemistry, University of Neuchâtel, 2000 Neuchâtel, Switzerland; mathilde.monachon@unine.ch (M.M.); sathiyanarayanan.ganesan@unine.ch (S.G.)
[2] Laboratoire de Conservation-Restauration Arc'Antique, 44300 Nantes, France; charlene.pele-meziani@loire-atlantique.fr
[3] Haute Ecole Arc Conservation Restauration, University of Applied Sciences and Arts Western Switzerland HES-SO, 2000 Neuchâtel, Switzerland; sabine.deweck@he-arc.ch
[4] Archaeological Service of Canton Bern, 3001 Bern, Switzerland; friederike.moll-dau@be.ch
[5] Swiss National Museum, Collection Center, 8910 Affoltern am Albis, Switzerland; janet.schramm@nationalmuseum.ch (J.S.); katharina.schmidt-ott@nationalmuseum.ch (K.S.-O.)
* Correspondence: edith.joseph@he-arc.ch or edith.joseph@unine.ch

Abstract: An innovative bio method was investigated to extract harmful iron and sulfur species from waterlogged wood samples. The method was compared with a chemical treatment. Both approaches were applied on lacustrine and marine samples, from different wood genera, to evaluate the versatility of the proposed bio method. Non-invasive and non-destructive methods were carried out to investigate both bio-based and chemical treatments. The result was that some wood genera were more affected by the bio approach, with a clear distinction between lacustrine beech and pine against oak and lime wood species. The chemical approach showed potential harm for the wooden structure, with acidic pH values and an increase of maximum water content, both implying degradation of the wood structure. In terms of extraction, no iron or sulfur products were detected by Raman spectroscopy on biologically treated samples, in agreement with extraction rates calculated. It was also suggested that iron bonded to wood was extracted with the chemical approach, and calcium content affected by both approaches.

Keywords: waterlogged wood; bio-based treatment; burial environment; wood; iron sulfides; extraction method; stabilization

Citation: Monachon, M.; Pelé-Meziani, C.; Ganesan, S.; de Weck, S.; Moll-Dau, F.; Schramm, J.; Schmidt-Ott, K.; Joseph, E. Assessing the Versatility of Bioextraction to Preserve Waterlogged Wood. *Forests* **2023**, *14*, 1656. https://doi.org/10.3390/f14081656

Academic Editor: Petar Antov

Received: 14 July 2023
Revised: 11 August 2023
Accepted: 14 August 2023
Published: 16 August 2023

1. Introduction

Several ways of degradation for wood material exist, all altering the mechanical performances of wood. Those damages can come from the chemical or biological factors of a specific environment. Exposure to changing atmospheric agents (relative humidity, temperature, and sunlight) induces slow degradation, in particular of the moisture content of wood [1,2]. The surrounding environment also affects the biological degradation of the wood material. For instance, fungi and insects develop mainly on wood material in urban or forestry environments, while bacteria occur more in a water environment [3]. When wood is found in anoxic conditions (i.e., low oxygen content, little UV-light exposition, high relative humidity), it is generally filled with water. This wood is called waterlogged wood.

Waterlogged objects have the particularity of maintaining an excellent shape, even though they were actively degraded by bacteria. Three main waterlogged environments exist: terrestrial, lacustrine, and marine. Even if the environmental conditions differ (pH, salts), waterlogged wood presents the same characteristics in the three environments: high water content, structural shape maintained, cell bacterial degradation, and contamination with sulfur and/or iron species [4,5]. Biodegradation for waterlogged wood consists of an

initial degradation by erosion bacteria. These primary degraders enter the wood through rays and pits and convert the crystalline cellulose content in secondary cell walls into an amorphous substance. Erosion bacteria do not affect the lignin content within wood middle lamellae [6]. Sulfate-reducing bacteria are secondary degraders of waterlogged wood. They interact with the sulfate ions (SO_4^{2-}) of the surrounding environment to form gaseous hydrogen sulfide (H_2S) [6–8]. H_2S fills the decayed cells of wood and different reactions can then occur. H_2S can either bound to wood and form organosulfur compounds, or it could react by corroding present metallic iron pieces, leading to the accumulation of iron sulfides within the wood cells [9–11].

This latter reaction is of great importance as it is the main issue encountered with the preservation of archaeological objects made of wood. If waterlogged archeological wood objects have conserved a proper shape in anoxic conditions, once recovered and exposed to a higher oxygen level and different relative humidity, the water starts to evaporate from the wood cells, leading to a collapse of the structure, and the iron sulfides oxidize to form iron oxides, iron sulfates, and sulfuric acid, weakening the mechanical properties of wood [4]. The oxidized iron compounds expand in volume in the cells and cracks can appear. Formation of sulfuric acid enhances a degradation of wood components, through an acidic hydrolysis of cellulose [12]. Furthermore, iron ions present in waterlogged wood are involved in the Fenton reaction which also induces the degradation of wood structures [13,14]. Therefore, for many years, waterlogged archaeological wood objects have been conserved in specialized laboratories with specific consolidating agents before drying [15,16]. However, even after consolidation of the wood artifacts, generally with polyethylene glycol (PEG), some degradation still occurs, especially when iron ions are present in a moist environment and form oxidative radicals deteriorating PEG [17].

To prevent the damage related to the presence of sulfur and iron species, many treatments have been developed and applied on waterlogged archeological wood. The use of strong complexing agents such as ethylenediamine tetraacetic acid (EDTA) or derivatives are the most efficient in terms of iron uptake [18–21]. However, discoloration of the surface as well as swelling of the structure are reported [19]. Concerning sulfuric acid neutralization, employment of alkaline baths allows one to reach a neutral pH at the surface of the treated objects [22], but also, the use of alkaline-earth carbonates and/or hydroxides or strontium nanoparticles, for instance [23–25]. Yet, these methods are long-time processes and could be harmful for the user and the environment. Therefore, research has turned toward more green and eco-friendly approaches.

For instance, molecules with similar structures of EDTA have been synthesized and present potential for an alternative eco-friendly iron complexation [26]. Some laboratories also suggested to encapsulate the harmful iron sulfides within the wood instead of extracting them as they are part of the objects' history [27]. A new trend is also emerging, by employing microorganisms to develop bio-based methods. Microbial siderophores (Desferoxamine) and sulfur-oxidizing bacteria (*Thiobacillus denitrificans*) were employed to extract iron and sulfur species from waterlogged lacustrine wood samples [15,28]. The result was that the preventive bio approach was as efficient as a benchmark chemical extraction method, with no alteration of the wooden structure. Based on the promising results of this innovative green approach, four wood genera were then investigated, coming from marine and lacustrine environments, to determine if such a preventive approach is versatile, or if its efficiency depends on the wood genus, burial environment, degree of wood degradation.

2. Materials and Methods

2.1. Waterlogged Wood Samples

The wood poles used in this study came from several lacustrine and marine sites in Switzerland (Neolithic period) and France (Roman period). They were provided by the three archaeological conservation departments: Arc'Antique (AA), Nantes, France; Archaeological Service of Bern Canton (ADB), Bern, Switzerland; and Swiss National Museum

(SNM), Affoltern am Albis, Switzerland. The wood materials collected are presented in Table 1.

Table 1. Characteristics of the wood samples collected from Arc'Antique (AA), Archaeological Service of Bern Canton (ADB), and Swiss National Museum (SNM) and set labelling used for the study: O for oak, M for model oak, FP and SP for freshwater and seawater pine, respectively, B for beech and L for lime.

Genus	Type of Wood	Location	Sets
Oak (*Quercus* sp.)	Hardwood	Saint-Lupien, Rezé, Nantes, FR	O-AA
		Hölzer campus, Lake Biel, Biel, CH	O-ADB
		Bevaix, Neuchâtel, CH	O-SNM
		Taüffelen, Lake Biel, Biel, CH	M-AA
		Taüffelen, Lake Biel, Biel, CH	M-ADB
Pine (*Pinus* sp.)	Softwood	Hölzer campus, Lake Biel, Biel, CH	FP-ADB
		DRASSM (unidentified site), Nantes, FR	SP-AA
Beech (*Fagus* sp.)	Hardwood	Taüffelen, Lake Biel, Biel, CH	B-ADB
Lime (*Tilia* sp.)	Hardwood	Opera, Zurich, CH	L-SNM

The poles were cut in slices of 2 cm thickness. Cubes of 2 × 2 × 2 cm were cut from the outer parts of the slices to have high and homogeneous degree of degradation. All cubes present the three transversal (Tv), tangential (Tg), and radial (Rd) wood sections.

For each wood set, 18 cubes were prepared and distributed randomly in three groups of 6 cubes. Six cubes were either biologically (BT) or chemically treated (CT), and six were left untreated (NT). In addition, six cubes per set were stored as reference material.

Some sets (M-AA and M-ADB) were artificially contaminated with iron and sulfur species as model samples. For M-AA, waterlogged oak wood samples were immersed in iron acetate 0.015 M solution (2 L, pH = 4.6). Stirring was achieved for 2 h before adding 200 mL of $Na_2S{\cdot}9H_2O$ 0.4 M. The samples were then left immersed at room temperature for 24 h. This protocol is adapted from Lennie et al. [29]. Concerning M-ADB, fresh oak samples have been previously buried in the lake Biel sediments, where the presence of sulfur-reducing bacteria was ascertained. The samples were placed inside a holed plastic box together with pieces of iron for 4 years, allowing the production of model samples artificially contaminated in a natural site.

2.2. Selection of Complexing and Oxidizing Agents

Siderophores are small microbial molecules produced by microorganisms in an iron-deficient environment [30,31]. They present one of the highest affinities for ferric ions, even greater than EDTA and its derivatives, forming very stable iron-siderophore complexes [32–34]. Commercial Desferoxamine (DFO, Novartis®) was selected for this study as iron chelator. *Thiobacillus denitrificans* was selected to oxidize reduced sulfur compounds. This strain is a facultative anaerobe bacteria growing at neutral pH and room temperature, classified as a non-pathogenic strain, and with the capacity to use reduced sulfur as a growing source [35–37].

In comparison, sodium persulfate ($Na_2S_2O_8$) was employed as a sulfur-reducing agent, and EDTA as an iron chelator, as reported in the literature [38].

2.3. Extraction Methods

Both bio and chemical extraction methods are a two-step protocol at room temperature under atmospheric pressure. Concerning the bio extraction (BT), 6 samples per set were first immersed for 10 days in DFO, with a concentration of 84 mM; then, the samples were rinsed with deionized water before being incubated for 20 days with the strain *T. denitrificans* (DSMZ 12475), cultivated according to standard anaerobic technics. For a chemical approach (CT), 6 samples per set were immersed in a solution of $Na_2S_2O_8$ 0.1 M

for 1 day, then rinsed before being immersed for 7 days in a solution of EDTA 0.125 M. All the extraction volumes were set at 250 mL. In parallel, 6 cubes per set remained in deionized water, as untreated samples (NT).

2.4. Analytical Protocol

Non-invasive and non-destructive methods were carried out directly on the different faces of 2 × 2 × 2 cm wood cubes, according to transversal (Tv), tangential (Tg), and radial (Rd) wood sections.

2.4.1. Colorimetry

Colorimetric coordinates (L*, a*, b*) in the CIELab color space were measured on the wood samples before and after extraction. Measurements were performed with a Konica Minolta CM-2600d Spectrophotometer, at the center of three faces (Tv, Tg, Rd) through plastic film to avoid contact between waterlogged wood and spectrophotometer window. The color variation was calculated according to the formula $\Delta E^* = \sqrt{(\Delta L^*)^2 + (\Delta a^*)^2 + (\Delta b^*)^2}$ where L* is the brightness and a* and b* the coordinates in the green to magenta and yellow to blue scale, respectively. The mean color variation was calculated and associated with its standard error.

2.4.2. pH

pH was measured at the surface of the wood samples with a surface electrode (flat membrane electrode 6.0256.100), before and after extraction. The pH of the extraction solutions was measured at the beginning and end of each extraction step. pH measurements were acquired with a 691 Metrohm standard pHmeter, calibrated with standard buffer solution pH = 4 and pH = 7.

2.4.3. Maximum Water Content

- The determination of Maximum Water Content (Umax) gives the weight proportion of wood substance to water in a sample completely filled with water. Umax is expressed as the weight of the water as a percentage of the weight of the dry wood substance [39]. MWC can therefore be considered to be directly proportional to the amount of decay. According to Macchioni et al. [39], the comparison with the values for sound wood shows the decrease in density. WW can be classified into five classes, reflecting the state of degradation. The loss of substance is reflected by a corresponding increase of the MWC, but as the value does not include the original dry density of the wood, different samples with identical MWC can present different stage of degradation, due to different initial density [40]. This classification is therefore indicative and not absolute.

Samples were classified according to their Umax values into 5 categories [39]:

- Grade 0: Umax < 135%—absence of decay
- Grade 1: 135 < Umax < 225%—initial decay
- Grade 2: 225 < Umax < 350%—advanced decay
- Grade 3: 350 Umax < 500%—important decay
- Grade 4: Umax > 500%—high decay

Before weighting, all samples were submitted to 2 cycles of 20 min vacuum. A container filled with deionized water was then placed on a weighting scale and the sample weight was measured with a sample suspended in air (W_{air}) or immersed in water (W_{water}). Umax was calculated according to the formula $\mathrm{Umax}(\%) = \frac{W_{air} - 3W_{water}}{3W_{water}} \times 100$.

2.4.4. Attenuated Total Reflectance Fourier Transformed Infrared Spectroscopy

Infrared spectra were recorded with a Nicolet iS5 spectrometer, with a diamond ATR accessory, and the following settings: 16 scans, spectral resolution of 4 cm^{-1}, wavenumber range of 4000–400 cm^{-1}, area of analysis of 62 µm. Two samples per set per treatment

were analyzed and three faces investigated (Tv, Tg, Rd). For each face, three spectra were acquired along the diagonal with v9.2.86 OMNIC software.

The spectra were processed with the v1.2.16 Spectragryph software. After baseline correction, the band at 1050 cm^{-1} was set at 1 to normalize spectra and the intensity of bands at 1158 and 1506 cm^{-1} listed. These bands are assigned to holocellulose and lignin content, respectively [41–43]. The degree of degradation was evaluated by calculating the ratio R1 = 1158/1506 and compared before and after extraction [44,45].

2.4.5. Raman Spectroscopy

Raman spectra were acquired with a Renishaw LabRam Aramis Horiba, with the following parameters: 632.8 nm laser, 100–2000 cm^{-1} range, 100× objective, 1800 lines/mm grating, 1000 µm confocal pinhole, 100 µm spectrometer entrance slit, 10% of laser power (0.99 mW at the surface of the sample). Two samples per set per treatment were analyzed and three faces investigated (Tv, Tg, Rd). Short acquisitions (5 accumulations of 10 s) were performed at the center of faces Tg and Rd, while long acquisitions (10 accumulations of 25 s) were carried out at the center of face Tv.

The spectra were processed with v1.2.16 Spectragryph software for baseline, SVN correction, and normalization.

2.4.6. X-ray Fluorescence

X-ray fluorescence (XRF) spectra were recorded with a portable Tracer 5 g XRF spectrometer (Bruker), with the following parameters: 20 kV, 60 µA, no filter, Spectral Mode, 60 s acquisition and window aperture of 3 mm. Two samples per set per treatment were analyzed and three faces investigated (Tv, Tg, Rd). For each face, one spectrum was acquired at the center of the faces.

The spectra were processed with v1.2.16 Spectragryph software. After baseline correction, the band at 2.69 keV (Rh) was set at 1 for normalization and the intensity of bands of sulfur S (2.31 keV), calcium Ca (3.70 keV), and iron Fe (6.40 keV) listed. Their intensities were compared before and after treatment.

2.5. Statistical Validation

In order to better assess the obtained results, experimental data were statistically analyzed using v 3.6.3. Rstudio software. Measured values were tested by Shapiro–Wil normality test. Then Principal Component Analysis (PCA) and two-way analysis of variance (ANOVA) were performed to determine statistical differences between the extraction protocols, as well as which variables affect the most the extraction results (Table 2). Significance was established at a *p*-value level of 0.05. Tukey's HSD significance was applied to find which significance variables affected most the study.

Table 2. Variables evaluated for the validation of alternative bio extraction method.

Genus	Burial Environment	Treatment Applied
Oak Pine Beech Lime	Lacustrine Marine	BT (biological) CT (chemical) NT (untreated)

3. Results

3.1. Samples Appearance

In general, the samples showed a dark appearance after each extraction treatment, similar to the one of untreated samples. The highest variations for BT sets were observed on lacustrine pine and beech (Figure 1, FP- and B-ADB).

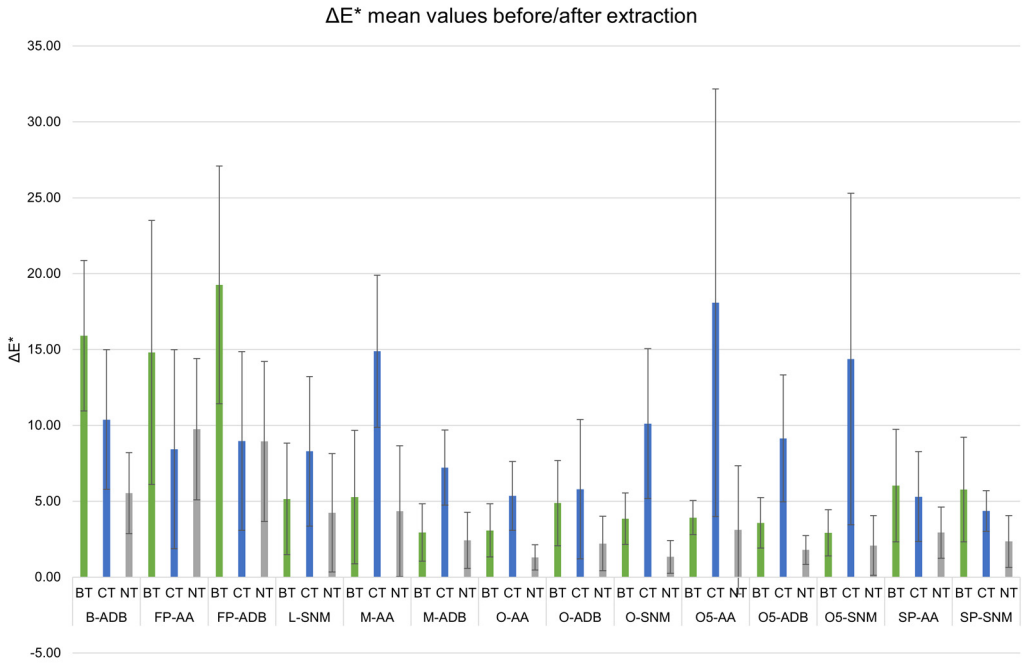

Figure 1. Mean color variation (ΔE*) between before and after extraction for biologically (BT, green) and chemically (CT, blue) treated sets, compared with untreated (NT, grey) samples, with standard error. Black line indicates the threshold of eye-perceivable color variation (ΔE* = 5).

For all the other wood sets, CT-samples generally had the highest ΔE* mean values. The chemical approach tended to modify more the wood samples appearance than the biological approach. It could be noticed that CT ΔE* mean values were almost all above ΔE* = 5, the threshold for the human eye to perceive a change in color [46].

According to ANOVA, significant statistic differences were observed for the variables wood genus ($f(3) = 98.95$, $p < 0.05$) and treatment ($f(2) = 20.695$, $p < 0.05$), with their interaction being significant. Burial environment did not present statistical significance ($f(1) = 0.140$, $p = 0.7083$). A Tukey post-hoc test validated significant pairwise differences between untreated (NT) and treated (BT and CT) samples, but also between some wood genus (i.e., Lime vs. Beech, Oak vs. Beech, Lime vs. Pine, Oak vs. Pine).

3.2. Wood Integrity

pH, Umax, and ATR-FTIR results were investigated to determine if any degradation occurred during extraction.

pH values remained in a neutral range for BT and NT samples while the value dropped at the end of the CT approach (Table 3). This was due to the pH of CT extraction solutions, which were acidic (pH between 1.8 and 4.3) while BT extraction solutions were slightly acidic (pH between 5.4 and 6.5). The only exception was set SP-AA, which originally presented an acidic pH.

Based on Umax values, the samples generally remained in the same degradation category. The only exceptions were L-SNM-CT, O-ADB (NT, BT & CT sets), and O-SNM (BT & CT samples). These samples ranked in an above degradation category after extraction. In addition, ATR-FTIR ratios highlighted that the values generally decreased for BT and NT samples compared to ratios before extraction (Table 3, Ref), while CT-samples values tended to increase. ANOVA validated the significance differences for treatment ($f(2) = 66.989$, $p < 0.05$) but not for wood genus ($f(3) = 1.483$, $p = 0.218$) or burial environment ($f(1) = 2.316$, $p = 0.129$). Tukey post hoc tests revealed significant pairwise differences between CT and BT samples and between NT and CT samples, but none between wood genera.

Table 3. Comparison of pH, Maximum Water Content (Umax), and ATR-FTIR holocellulose/lignin ratio (R1 = 1158/1506) values before (Ref) and after biological (BT) and chemical (CT) extraction methods, compared with untreated (NT) samples, with standard error in brackets.

Set	Treatment	pH	Umax	R1
B-ADB	Ref	6.96 (±0.1)	4	0.52 (±0.1)
	BT	5.71 (±0.2)	4	0.47 (±0.1)
	CT	3.23 (±0.1)	4	0.48 (±0.1)
	NT	6.40 (±0.3)	4	0.81 (±0.1)
FP-ADB	Ref	6.47 (±0.4)	4	0.38 (±0.1)
	BT	5.12 (±0.2)	4	0.41 (±0.1)
	CT	2.55 (±0.2)	4	0.47 (±0.1)
	NT	5.86 (±0.2)	4	0.40 (±0.1)
L-SNM	Ref	6.61 (±0.1)	2	0.57 (±0.2)
	BT	6.60 (±0.2)	2	0.57 (±0.1)
	CT	3.37 (±0.2)	4	0.46 (±0.1)
	NT	5.77 (±0.4)	2	0.53 (±0.1)
M-AA	Ref	5.51 (±0.3)	4	0.25 (±0.1)
	BT	5.81 (±0.3)	4	0.41 (±0.1)
	CT	2.76 (±0.0)	4	0.39 (±0.1)
	NT	4.58 (±0.1)	4	0.31 (±0.1)
M-ADB	Ref	6.87 (±0.2)	1	0.68 (±0.1)
	BT	6.19 (±0.2)	1	0.63 (±0.2)
	CT	3.31 (±0.4)	1	0.89 (±0.2)
	NT	6.11 (±0.4)	1	0.60 (±0.2)
O-AA	Ref	6.75 (±0.3)	4	0.37 (±0.1)
	BT	6.36 (±0.5)	4	0.36 (±0.2)
	CT	2.92 (±0.2)	4	0.47 (±0.2)
	NT	6.42 (±0.4)	4	0.35 (±0.1)
O-ADB	Ref	6.27 (±0.2)	3	0.69 (±0.2)
	BT	5.67 (±0.3)	4	0.45 (±0.1)
	CT	2.77 (±0.1)	4	1.00 (±0.3)
	NT	5.80 (±0.2)	4	0.50 (±0.1)
O-SNM	Ref	6.48 (±0.1)	2	0.61 (±0.2)
	BT	6.32 (±0.1)	3	0.63 (±0.2)
	CT	3.11 (±0.1)	3	0.45 (±0.2)
	NT	5.79 (±0.5)	2	0.65 (±0.2)
SP-AA	Ref	2.50 (±0.2)	4	0.39 (±0.2)
	BT	5.88 (±0.3)	4	0.47 (±0.1)
	CT	2.39 (±0.1)	4	0.52 (±0.1)
	NT	2.50 (±0.1)	4	0.50 (±0.2)

3.3. Efficiency of Extraction

At last, the presence of iron and sulfur was investigated to evaluate if the proposed innovative bio extraction method was an efficient alternative to the chemical method.

Before extraction, corrosion compounds were identified. Artificially contaminated oak model samples (M-AA) presented bands at 247, 299, and 384 cm^{-1}, and at 152, 220, and 473 cm^{-1}, assigned to goethite (α-FeOOH) and to elemental sulfur (α-S_8), respectively [47,48]. Lacustrine pine (FP-ADB) also presented bands at 137, 195, 395, and 518 cm^{-1}, attributed at titanium oxide, probably under anatase form (TiO_2) [49]. After extraction, α-FeOOH, α-S_8, and TiO_2 were still identified, in particular on M-AA and SP-AA samples either chemically treated or untreated. Chemically treated SP-AA samples also presented bands at 480 and 508 cm^{-1}, probably due to the presence of ferromanganese minerals [50,51]. According to Raman spectroscopy, no corrosion products were present on biologically treated samples. Other bands were detected and attributed to wood components [41,52]. A particular attention was given at the bands around 1450 and 1490 cm^{-1},

as they could be assigned to cellulose and lignin content, respectively [52], or iron–tannin complexes [53]. It was observed that the band at 598 cm^{-1} for BT and NT samples shifted to 571 cm^{-1} for CT samples, and that the band at 1490 cm^{-1} decreased in intensity for CT samples while it remained intense and sharp for BT and NT samples (Figure 2). This could give further information regarding the wood structure, or the compounds extracted.

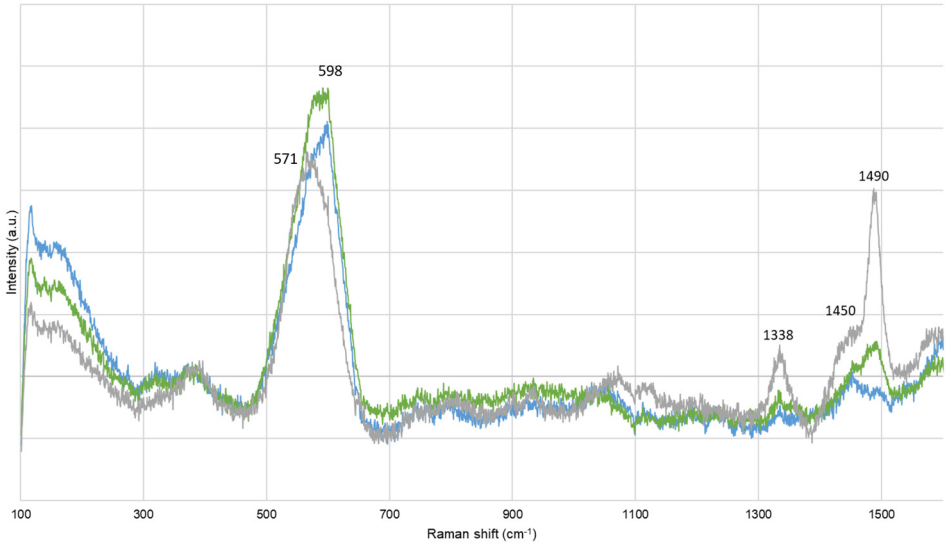

Figure 2. Representative Raman spectra for sets biologically (green) and chemically (blue) treated, compared with untreated (grey) samples.

Further investigations were performed with XRF. The intensities of iron and sulfur bands were compared, before and after extraction. Extraction rates were calculated to evaluate the efficiency of the method at the samples 'surface level (Table 4).

Table 4. Iron and sulfur extraction rates based on the XRF band intensities at the surface of wood samples after biological (BT) and chemical (CT) extraction method, compared with untreated (NT) samples, with standard error in brackets.

Set	Treatment	Iron Extraction Rate (%)	Sulfur Extraction Rate (%)
B-ADB	BT	23.55 (±5.8)	21.15 (±6.7)
	CT	27.48 (±5.9)	0.00 (±0.0)
FP-ADB	BT	51.28 (±19.3)	15.54 (±6.7)
	CT	52.34 (±0.3)	10.49 (±1.6)
L-SNM	BT	47.98 (±20.8)	24.42 (±8.5)
	CT	67.58 (±2.6)	8.98 (±1.9)
M-AA	BT	96.13 (±2.4)	80.44 (±7.8)
	CT	70.55 (±28.1)	68.71 (±17.3)
M-ADB	BT	50.69 (±25.7)	27.47 (±5.9)
	CT	54.95 (±15.4)	0.00 (±0.0)
O-AA	BT	66.67 (±22.4)	41.76 (±11.0)
	CT	54.37 (±23.1)	10.71 (±7.5)
O-ADB	BT	54.22 (±19.5)	16.29 (±7.5)
	CT	61.10 (±11.4)	15.73 (±2.2)
O-SNM	BT	36.77 (±4.8)	15.97 (±2.7)
	CT	34.80 (±12.0)	0.00 (±0.0)
SP-AA	BT	65.04 (±19.3)	28.55 (±10.3)
	CT	52.34 (±0.3)	18.11 (±6.5)

Concerning iron, both CT and BT methods presented important extraction rates, in the same range. Sulfur extraction rates were not as important as iron. Yet, the rates were higher for BT samples than CT samples. ANOVA showed no significant difference for treatment (f(1) = 0.90, p = 0.345), wood genus (f(3) = 1.325, p = 0.271), or burial environment (f(1) = 0.278, p = 0.599) (Table 5).

Table 5. Two-way ANOVA table for iron and sulfur extraction rates considering the wood genus, treatment applied, and the burial environment.

Species	Effect	Sum Sq	Mean Sq	df	F Value	p-Value
Iron	Genus (a)	20,338	6779	3	3.661	0.0149
	Treatment (b)	10	10	1	0.006	0.9407
	Environment (c)	13,146	13,146	1	7.095	0.0090
	a × b	11,129	376	3	0.203	0.8939
	a × c	7806	7806	1	4.802	0.0307
	b × c	800	800	1	0.432	0.51267
Sulfur	Genus (a)	1670	557	3	1.454	0.231
	Treatment (b)	5965	5965	1	1.556	0.2150
	Environment (c)	5424	5424	1	1.415	0.2369
	a × b	2750	917	3	0.223	0.880
	a × c	11,236	11,236	1	2.879	0.0928
	b × c	10,639	10,639	1	2.776	0.0987

Based on analysis of iron and sulfur extraction rates, one can observe that the wood genus and the burial environment variables and their interaction affect the iron extraction rate (p-value < 0.05), while none of the evaluated variables seemed to impact the sulfur extraction rate (p-value > 0.05).

Both Raman and XRF analyses demonstrated the potential of BT as an alternative extraction method to preserve waterlogged wood.

4. Discussion

An innovative bio extraction protocol was evaluated during this study, as an alternative method to current chemical approaches to pretreat waterlogged wood before further conservation treatments. The goal of this study was to determine if this two-step bio extraction, already carried out of some lacustrine oak and pine wood [15,28], could be applied for any wood genus, also from different burial environments. The performances of the proposed bio extraction method were evaluated in terms of iron and sulfur extraction efficiency as well as innocuousness towards wood integrity. In addition, the results obtained with model samples are discussed to ascertain the accuracy of model samples to replicate the behavior of waterlogged archaeological wood.

4.1. Iron Extraction Efficiency

The current extraction treatments applied on waterlogged wood are not based on wood genus, but mainly on the degree of degradation and contamination with iron and sulfur species. However, wood has a complex structure, which differs from hardwood to softwood. For instance, their cellulose or lignin content varies, but also inorganic and ashes content. Among the same genus, some disparities also exist, making each wood tree unique [54]. Another important constituent in wood is tannins (i.e., polyphenol compounds). It was reported that the oak wood genus contains more tannin than other genera [55]. Among diverse properties, tannins give wood its color [1]. Between all sets studied here, oak sets presented the darkest hue, independently from their burial sites (i.e., lacustrine vs. marine), and lacustrine beech and pine wood genera were the sets presenting a less dark appearance. The dark coloration of oak sets (i.e., O-AA, O-ADB, and O-SNM) may come from the formation of iron–tannin complexes (Fe-Tan). Such complexes have been reported as giving a black appearance to wood [56,57]. This hypothesis is validated by the presence

of Raman bands around 1338, 1450, 1490, and 1578 cm^{-1} on untreated samples (Figure 2, grey spectrum) [52]. Those bands were also observed for beech, lime, and pinewood, but with lower Raman intensities:

O-SNM > M-ADB > O-ADB > O-AA > M-AA > SP-AA > B-ADB > FP-ADB > L-SNM

It was also reported in many literature that waterlogged archeological wood presents a characteristic dark hue, due to the accumulation of iron from metallic pieces [54,58], or bacterial activity [59]. Indeed, even if lime samples showed the lowest Raman intensity for the Fe-Tan band, this set had important iron content, according to XRF measurements:

M-AA > O-SNM > M-ADB > O-ADB > SP-AA > O-AA > L-SNM >> FP-ADB > B-ADB

After extraction, CT samples presented the highest color variation (Figure 1, blue bars). This color variation can be related to the decrease of the Raman band at 1490 cm^{-1} observed for all CT samples. The decrease of this Raman band implies that the content of Fe-Tan complexes diminished on the treated surface. Therefore, not only were iron sulfides compounds extracted during the chemical approach, but also Fe-Tan complexes. According to Perron and Burmagim and Rapti et al. [33,60], Fe-Tan and Fe-EDTA have stability constant within the same range. Perron and Burmagim have conducted complexation studies of iron with both tannic acid and DTPA (diethylenetriamine pentaacetic acid) [60]. They noticed that not all the Fe-Tan complexes were dissolved when the wooden samples were immersed in DTPA solutions. Therefore, even strong complexing agents cannot totally extract all iron species from waterlogged wood. Based on the XRF extraction rates calculated, iron extraction rates varied between 27% and 71% with the CT method. Some iron species thus remained within the treated samples, as observed with Raman spectroscopy with the presence of iron oxyhydroxides still detected after extraction. Concerning the BT approach, it is well documented that siderophores Desferoxamine DFO have a stronger stability constant toward iron than EDTA according to Rapti et al. [33]. This complexing agent could then be more efficient toward iron extraction from waterlogged wood. From the Raman spectra, no corrosion products were identified on any BT samples, and the XRF extraction rates were superior to CT ones (23%–96% range). These two results highlighted the great potential of the biological approach studied. Yet, the band attributed to Fe-Tan was still visible after BT extraction, less intense than for NT samples but implying that Fe-Tan complexes were less removed than by CT extraction. This result could also imply low alteration and that wood structure is preserved after BT extraction. A question about Fe-Tan stability over-time is raised, especially if the samples are then consolidated with PEG. Indeed, the presence of iron inside consolidated waterlogged wood samples can enhance new degradation processes. The PEG hygroscopicity favors the formation of iron ions, which can further oxidize the PEG polymer through the Fenton reaction, inhibiting the consolidation purpose of PEG [61]. In addition, those iron ions could continue a cellulosic degradation, endangering the wood structure [62]. Further investigation regarding Fe-Tan complexes' possible oxidation and wood degradation consolidated with PEG should be considered.

4.2. Sulfur Extraction Efficiency

Sulfur species are also harmful for waterlogged wood artifacts, as oxidation of reduced sulfur compounds could lead to acidification, and therefore, to slow deterioration of waterlogged wood artifacts [5,63,64]. Though sulfur content was less important than iron according to XRF analyses, all sets were contaminated with sulfur. Elemental sulfur was identified by Raman spectroscopy on model oak samples (M-AA) before treatment and still detected on CT and NT samples after treatment. This result on artificially contaminated samples showed the potential of the bio approach compared to the chemical one to extract sulfur species. This is validated with the XRF results, where sulfur extraction rates of BT were superior to CT (15%–81% vs. 0%–69%, respectively). The strain *Thiobacillus denitrificans* already proved its ability to oxidize iron sulfides compounds [36,37,65–67]. If first applied in power supply to prevent corrosion [35,68], *T. denitrificans* was also exploited for its unique properties in the field of conservation–restoration and proved efficiency on

waterlogged wood without affecting the wooden matrix [69]. Mackinawite (FeS), pyrite (FeS_2), and sulfur (S_0) can be growth sources for *T. denitrificans* [36,70]:

$$5FeS + 8NO_3^- + 8H^+ \rightarrow 5Fe^{2+} + 5SO_4^{2-} + 4N_2 + 4H_2O$$
$$5FeS_2 + 14NO_3^- + 4H^+ \rightarrow 5Fe^{2+} + 10SO_4^{2-} + 7N_2 + 2H_2O$$
$$17S_{(0)} + 24NO_3^- + 8H_2O \rightarrow 17SO_4^{2-} + 6NO_2^- + 9N_2 + 16H^+$$

The absence of elemental sulfur from biologically treated samples proved that this compound was oxidized during the extraction time with *T. denitrificans*. Moreover, this strain can be motile thanks to its polar flagellum, allowing the penetration of wood through pores and fibers [67]. ESEM analyses performed in previous studies validated the ability of *T. denitrificans* to reach the wood core and to convert the reduced sulfur compounds into sulfates [69]. Based on these results and sulfur extraction rates of the current study, one could hypothesize that *T. denitrificans* could penetrate deeper than sodium persulfate $Na_2S_2O_8$. Indeed, this chemical was suggested to improve the sulfur extraction from waterlogged wood [38]. Yet, the sulfur extraction rates with the CT approach were less important [27,28]. For some sets, the extraction rate was zero (Table 4). Sets presenting no sulfur extraction were from a lacustrine environment. Yet, contrary to iron where the wood genus and the burial environment affected the extraction rates (Table 5), two-way ANOVA showed that none of the evaluated variables impacted the sulfur extraction rates. Hence, $Na_2S_2O_8$ performance toward sulfur oxidation was not affected by the burial environment, and its efficiency was lower than the bacterial approach. In addition, statistical approaches showed that the wood genus did not affect the sulfur extraction. Therefore, independently of the wood cells (i.e., vessels vs. tracheids), extraction solutions penetrated within the samples to promote sulfur reduction. However, the mobility of *T. denitrificans* could allow the bacteria to penetrate deeper than $Na_2S_2O_8$ and, so, to oxidize more reduced sulfur species present in the wood core.

As Raman highlighted the presence of Fe-Tan complexes, different forms of sulfur could accumulate. Indeed, sulfur is not only present in waterlogged wood as elemental sulfur or iron sulfides, but also as organosulfur, bounded to the wood matrix [12,61]. They are found in lignin-rich parts of the wood and present a longer oxidation pathway than problematic iron sulfides [71]. Organosulfur could be discriminated via XANES spectroscopy or with the relative amounts of S/Fe [12]. In our study, S/Fe ranged between 0.02 and 0.49. They did not correlate with ratio to identify mackinawite S/Fe = 1, greigite S/Fe = 0.75, or pyrite S/Fe = 0.5. Therefore, organosulfur may have formed. Organosulfur has a strong interaction with the wood matrix [72,73] and, in particular, its encapsulation within lignin protects it from oxidation and, thus, wood from acidification [12,63]. Therefore, it is less accessible to oxidizing agents and could remain within waterlogged wood. As the samples were shaped from the outer layers of wood poles, their lignin content was higher than the carbohydrates one. Therefore, organosulfur compounds may have formed preferentially toward other reduced sulfur compounds, especially for model samples prepared in the laboratory. Indeed, the sulfur content of artificially contaminated samples is in the range of the other naturally aged sets, according to XRF analyses. Artificial contamination of wood did not thus increase sulfur content. In addition, XRF did not gave information of the speciation of measured elements, and it was then assumed that sulfur corrosion products were formed, as observed with Raman spectroscopy. However, this type of analysis is carried out on the surface, with the beam only penetrating within inside the wood subsurface. Aluri et al. observed that organosulfur was present in the majority after 1–12 mm [74]. Deeper analyses are needed to understand the interaction with sulfur and mechanisms occurring with the wood matrix.

Based on this study, most harmful iron and sulfur species were extracted from lacustrine and marine wood. Based on the wood genus investigated, the performance of the extractions differed, and optimization is required to develop a versatile bio extraction method. Long-term monitoring is planned, with an accelerated aging of the samples

with harsh conditions to determine if the remaining species oxidized, and to validate the innocuousness of the bio approach [75].

4.3. Innocuousness towards Wood Integrity

Wood degradation was observed with the evaluated protocols. According to the maximum water content (Umax) values, the sets remained in their degradation rates, with the exceptions of lacustrine lime and oak wood (Table 3). As for the color variation, one can observe a scission between the sets: Lime and Oak versus Beech and Pine. The variable wood genus is again placed in the spotlight with the analysis, highlighting the importance of characterizing wood artifacts before selecting appropriate treatment. Lacustrine lime and oak treated with the CT approach were the most degraded, according to Umax, as they ranked in the superior degradation category. This change of category implies that wood degradation occurred during the extraction time. Immersion in $Na_2S_2O_8$ and EDTA are the two steps of CT. Both the solutions presented acidic pH, sometimes lower than 2. In particular, $Na_2S_2O_8$ is known to degrade some organic compounds as well as possessing a bleaching power [76,77]. Phenolic compounds, such as lignin, are mainly affected by $Na_2S_2O_8$ action. An acidic hydrolysis of the lignin could then occur, explaining the observed increase of the ATR-FTIR holocellulose/lignin ratio values. Normally, lignin and holocellulose are not affected by complexing agents [21]. Yet, the pH measured in this research is acidic, while other studies referred to slightly alkaline pH. If this acidic pH may be harmful for the wood structure, it would be necessary to perform iron extraction in the best conditions according to the literature [78]. Lacustrine oak samples (O-ADB and O-SNM) changed Umax rank after application of the BT approach. This observation was supported by ANOVA and Tukey post-hoc tests, with a statistically significant difference between the wood genus, especially Lime and Oak versus Beech versus Pine.

When applying PCA (Figure 3), it resulted that the ATR-FTIR variables were not considered to cluster samples. This could imply that all samples selected for this study presented a similar degradation state, or that this approach is not the most pertinent for our purpose.

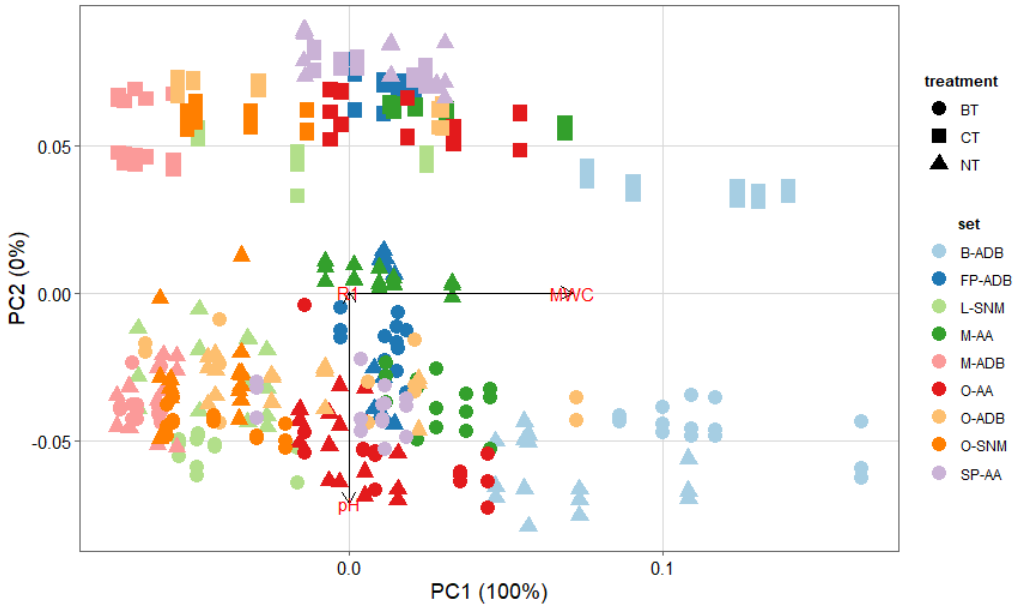

Figure 3. PCA plot for all sets biologically (circle, BT) and chemically (square, CT) treated, compared with untreated (triangle, NT) samples, for the degradation variables pH, maximum water content (Umax) and ATR-FTIR ratio (R1).

Nevertheless, additional PCA analysis highlighted the importance of the treatment chosen but also that Umax is the main variable to discriminate samples, as its weight is of 100% principal component PC1.

Closer examination of XRF spectra highlighted that the content in calcium varied between NT, BT, and CT samples. Calcium was observed on the wood samples prior to treatment, and in non negligeable proportions. According to Wiedenhoeft and Miller, calcium is mainly present within wood bark, i.e., the most outer layer of wood trunk, and could also affect the wood pH [1]. If not considered in the first study, the extraction of calcium was investigated here. Indeed, it was observed that after both extraction methods, the XRF band of calcium decreased in intensity. In his study, Norvell stipulated that EDTA has the capacity to complex both iron and calcium depending on the pH of the solution [78]. Fe-EDTA complexes formed for pH < 6.3, which is the case here, while Ca-EDTA are more stable for pH > 6.8. However, despite the acidic pH of the CT approach, calcium was extracted (13%–83% range). One hypothesis could be that iron and calcium compete for complexation or possibly all iron available was first chelated and then calcium-EDTA complexes were formed. When compared, the extraction rates for calcium were lower with the biological approach (0%–70%). This observation agreed with the literature review stipulating that the Ca-DFO stability constant is small compared to Fe-DFO [79]. Deeper investigation is required to fully understand the extraction of calcium as well as determining if removal of calcium species could affect waterlogged wood integrity on long term perspectives.

4.4. Representativity of Model Samples

In this study, two types of model samples were employed to test the proposed bio extraction. The aim of developing methods to mock up waterlogged wood is to have a large panel of samples to perform some tests, prior to application on a real case study.

It was interesting to observe the behavior of the model samples. The ones buried in Lake Biel for 4 years (M-ADB) presented the same characteristics as archaeological oak sets (O-ADB and O-SNM), with a dark appearance conserved after treatment, neutral wood pH, and R1 ratio in the same range. The only difference came from the Umax values. Indeed, if wood degradation was induced on the surface during these 4 years, the samples' core was still preserved. M-ADB samples are very hard, while O-ADB and O-SNM are soft. According to Umax, M-ADB presented an initial decay (rank 1) while O-ADB and O-SNM were classified as advanced and importantly decayed (Table 3). The comparison of M-ADB with O-ADB and O-SNM showed the potential of reburial to replicate waterlogged wood. Matthiessen et al. valorized the reburial in sites where the parameters are known to conserve archaeological iron objects in situ [80,81]. In our study, burial was used to induce degradation on fresh oak wood. Holocellulose degradation was enhanced but not complete. Lucejko et al. have worked for almost two decades on the monitoring of contemporary oak wood in lacustrine conditions [82–84]. It resulted from this study that the degradation state was very low, with mainly hemicellulose content affected. To reach the desired degree of degradation, our model samples should remain at least 20 years, or even more; or a preliminary degradation step could be applied on the fresh oak before burial. Concerning the degree of contamination, as for O-ADB and O-SNM, no iron sulfides products were identified with Raman spectroscopy, but iron and sulfur band intensities in XRF measurements were in the same range for M-ADB and O-ADB and O-SNM. Calculated iron and extraction rates were also in the same range as for O-ADB and O-SNM. This first approach to replicate waterlogged archaeological wood was encouraging and requires more research.

Concerning the second model samples M-AA, Neolithic lacustrine oak was selected as it already presents an important degree of degradation [85]. The samples were artificially contaminated to form iron sulfide compounds. Raman spectroscopy identified goethite and elemental sulfur, as iron and sulfur corrosion products and no iron sulfides, contrary to what was reported in the literature. Therefore, samples were effectively contaminated with iron

and sulfur, but the desired compounds were not formed. According to XRF analysis, M-AA had the highest iron content, with an average XRF band intensity four times superior to lacustrine oak samples, and sulfur content in the same range as the other sets. M-AA had also the highest extraction rates, probably due to the instability of the formed compounds compared to the naturally aged sets. As discussed in Sections 4.1 and 4.2, the BT approach was more efficient than the CT method to extract harmful iron and sulfur species. Concerning the state of degradation, M-AA samples were classified as highly decayed and with the lowest ATR-FTIR ratio (Table 3). In general, the pH and ratio values were lower for M-AA than the other oak sets (M-ADB, O-AA, O-ADB, O-SNM). If the contamination protocol was adapted to evaluate the extraction performance, it may have enhanced further wood degradation. This approach to producing model samples was performant in terms of contamination but may be not as representative when talking about wood integrity.

5. Conclusions

In this project, a preventive bio-based pre-treatment was investigated, prior to the conservation of fragile waterlogged archaeological wood objects. This study regarding the preservation of lacustrine and marine waterlogged wood with a bio approach highlighted the potential of this innovative extraction method, but mainly the importance of the type of wood objects treated. If harmful iron and sulfur species were extracted, the wood genus often affected the performance of the approach in terms of visual appearance and iron extraction rate. Generally, the burial environment did not affect the efficiency of the bio approach.

Different results were obtained when the bio extraction was compared to a chemical one, one method looking more appropriate for hardwood and the other for lacustrine beech and pinewood. Therefore, a bio extraction method has the potential for the preservation of waterlogged archaeological wood objects but optimization toward the wood genus is still required. Further investigation is ongoing to provide end-users with an optimized bio extraction protocol based on a gel formulation and aerobic bacteria that could be more easily handled. The environmental and economic aspects of biological and chemical protocols are also carefully considered, taking into account the production of the biological reagents to their final use (time of application, reiteration, etc.), comparative to the traditional use of sodium persulfate ($Na_2S_2O_8$) and EDTA.

Author Contributions: Conceptualization, E.J.; methodology, M.M., C.P.-M., S.G., K.S.-O., F.M.-D., J.S. and E.J.; software, M.M.; validation, M.M., S.G., K.S.-O., F.M.-D., J.S. and E.J.; formal analysis, M.M.; investigation, M.M., C.P.-M., S.d.W. and K.S.-O.; data curation, M.M.; writing—original draft preparation, M.M.; writing—review and editing, M.M., C.P.-M., K.S.-O. and E.J.; visualization, M.M.; supervision, E.J.; project administration, E.J.; funding acquisition, E.J. All authors have read and agreed to the published version of the manuscript.

Funding: This research was funded by the Swiss National Science Foundation (SNSF), grant number PP00P2_190081, 2020–2023.

Institutional Review Board Statement: Not applicable.

Informed Consent Statement: Not applicable.

Data Availability Statement: Not applicable.

Conflicts of Interest: The authors declare no conflict of interest.

References

1. Winandy, J.E.; Rowell, R.M. 11 chemistry of wood strength. In *Handbook of Wood Chemistry and Wood Composites*; CRC Press: Boca Raton, FL, USA, 2005; Volume 303.
2. Williams, R.S. Weathering of wood. In *Handbook of Wood Chemistry and Wood Composites*; CRC Press: Boca Raton, FL, USA, 2005; Volume 7, pp. 139–185.
3. Ibach, R.E. Biological properties. In *Handbook of Wood Chemistry and Wood Composites*; CRC Press: Boca Raton, FL, USA, 2005; pp. 99–120.

4. Wetherall, K.M.; Moss, R.M.; Jones, A.M.; Smith, A.D.; Skinner, T.; Pickup, D.M.; Goatham, S.W.; Chadwick, A.V.; Newport, R.J. Sulfur and iron speciation in recently recovered timbers of the Mary Rose revealed via X-ray absorption spectroscopy. *J. Archaeol. Sci.* **2008**, *35*, 1317–1328. [CrossRef]
5. Rémazeilles, C.; Saheb, M.; Neff, D.; Guilminot, E.; Tran, K.; Bourdoiseau, J.-A.; Sabot, R.; Jeannin, M.; Matthiesen, H.; Dillmann, P.; et al. Microbiologically influenced corrosion of archaeological artefacts:Characterisation of iron(II) sulfides by Raman spectroscopy. *J. Raman Spectrosc.* **2010**, *41*, 1425–1433. [CrossRef]
6. Björdal, C.G. Microbial degradation of waterlogged archaeological wood. *J. Cult. Herit.* **2012**, *13*, S118–S122. [CrossRef]
7. Fors, Y.; Jalilehvand, F.; Risberg, E.D.; Björdal, C.; Phillips, E.; Sandström, M. Sulfur and iron analyses of marine archaeological wood in shipwrecks from the Baltic Sea and Scandinavian waters. *J. Archaeol. Sci.* **2012**, *39*, 2521–2532. [CrossRef]
8. Nilsson, T.; Björdal, C. Culturing wood-degrading erosion bacteria. *Int. Biodeterior. Biodegrad.* **2008**, *61*, 3–10. [CrossRef]
9. Sandström, M.; Jalilehvand, F.; Persson, I.; Gelius, U.; Frank, P.; Hall-Roth, I. Deterioration of the seventeenth-century warship Vasa by internal formation of sulphuric acid. *Nature* **2002**, *415*, 893–897. [CrossRef] [PubMed]
10. Sandström, M.; Fors, Y.; Jalilehvand, F.; Damian, E.; Gelius, U. Analyses of sulfur and iron in marine-archaeological wood. In Proceedings of the Ninth ICOM Group on Wet Organic Archaeological Materials Conference, Copenhagen, Denmark, 7–11 June 2004; pp. 181–202.
11. Florian, M.L.E. Deterioration of organic materials other than wood. In *Conservation of Marine Archaeological Objects*; Elsevier: Amsterdam, The Netherlands, 1987; pp. 21–54.
12. Fors, Y.; Sandström, M. Sulfur and iron in shipwrecks cause conservation concerns. *Chem. Soc. Rev.* **2006**, *35*, 399–415. [CrossRef] [PubMed]
13. Emery, J.A.; Schroeder, H.A. Iron-catalyzed oxidation of wood carbohydrates. *Wood Sci. Technol.* **1974**, *8*, 123–137. [CrossRef]
14. Hrdlička, L.; Škulcová, A.; Ház, A. Degradation of lignin via Fenton reaction. In Proceedings of the 5th International Scientific Conference, Renewable Energy Sources, Tatranské Matliare, Slovakia, 20–22 May 2014.
15. Monachon, M.; Albelda-Berenguer, M.; Lombardo, T.; Cornet, E.; Moll-Dau, F.; Schramm, J.; Schmidt-Ott, K.; Joseph, E. Evaluation of an alternative biotreatment for the extraction of harmful iron and sulfur species from waterlogged wood. *Eur. Phys. J. Plus* **2021**, *136*, 937. [CrossRef]
16. Jensen, J.B. Vaccum freeze-drying managed by object temperature. In Proceedings of the 13th ICOM-Group on Wet Organic Archaeological Materials Conference, Florence, Italy, 16–21 May 2016; pp. 315–324.
17. Almkvist, G.; Persson, I. Degradation of polyethylene glycol and hemicellulose in the Vasa. *Holzforschung* **2008**, *62*, 64–70. [CrossRef]
18. Suryawanshi, D.G.; Bisaria, S.K. Removing metallic stains from paper objects using chelating agent EDTA. *Restaur. Int. J. Preserv. Libr. Arch. Mater.* **2005**, *26*, 276–285. [CrossRef]
19. Almkvist, G.; Persson, I. Extraction of iron compounds from wood from the Vasa. *Holzforschung* **2006**, *60*, 678–684. [CrossRef]
20. Pecoraro, E.; Pelé-Meziani, C.; Macchioni, N.; Lemoine, G.; Guilminot, E.; Shen, D.; Pizzo, B. The removal of iron from waterlogged archaeological wood: Efficacy and effects on the room temperature wood properties. *Wood Mater. Sci. Eng.* **2022**, *18*, 672–689. [CrossRef]
21. Almkvist, G. *Iron Removal from Waterlogged Wood*; Swedish University of Agricultural Sciences: Uppsala, Sweden, 2013.
22. Fors, Y.; Richards, V. The effects of the ammonia neutralizing treatment on marine archaeological Vasa wood. *Stud. Conserv.* **2010**, *55*, 41–54. [CrossRef]
23. Giorgi, R.; Chelazzi, D.; Baglioni, P. Nanoparticles of calcium hydroxide for wood conservation. The deacidification of the Vasa warship. *Langmuir* **2005**, *21*, 10743–10748. [CrossRef]
24. Giorgi, R.; Chelazzi, D.; Baglioni, P. Conservation of acid waterlogged shipwrecks: Nanotechnologies for de-acidification. *Appl. Phys. A* **2006**, *83*, 567–571. [CrossRef]
25. Schofield, E.J.; Sarangi, R.; Mehta, A.; Jones, A.M.; Smith, A.; Mosselmans, J.F.W.; Chadwick, A.V. Strontium carbonate nanoparticles for the surface treatment of problematic sulfur and iron in waterlogged archaeological wood. *J. Cult. Herit.* **2016**, *18*, 306–312. [CrossRef]
26. Onawole, A.T.; Hussein, I.A.; Nimir, H.I.; Ahmed, M.E.M.; Saad, M.A. Molecular Design of Novel Chemicals for Iron Sulfide Scale Removal. *J. Chem.* **2021**, *2021*, 7698762. [CrossRef]
27. Chaumat, G.; Zahnweh, D.; Martinez-Carballal, X.; Caillat, L.; Guiblain, T.; Dbeaurain, M. Development of curative and preventive treatments of waterlogged archaeological wood contaminated by pyrite. In Proceedings of the 14th ICOM-CC Wet Organic Archaeological Materials Conference, Portsmouth, UK, 20–24 May 2019.
28. Monachon, M.; Albelda-Berenguer, M.; Lombardo, T.; Cornet, E.; Moll-Dau, F.; Schramm, J.; Schmidt-Ott, K.; Joseph, E. Evaluation of Bio-Based Extraction Methods by Spectroscopic Methods. *Minerals* **2020**, *10*, 203. [CrossRef]
29. Lennie, A.R.; Redfern, S.A.T.; Schofield, P.F.; Vaughan, D.J. Synthesis and Rietveld crystal structure refinement of mackinawite, tetragonal FeS. *Mineral. Mag.* **1995**, *59*, 677–683. [CrossRef]
30. Saha, R.; Saha, N.; Donofrio, R.S.; Bestervelt, L.L. Microbial siderophores: A mini review. *J. Basic Microbiol.* **2013**, *53*, 303–317. [CrossRef] [PubMed]
31. Albelda-Berenguer, M.; Monachon, M.; Joseph, E. Siderophores: From natural roles to potential applications. *Adv. Appl. Microbiol.* **2019**, *106*, 193.

32. Rapti, S.; Boyatzis, S.; Rivers, S.; Velios, A.; Pournou, A. Removing iron stains from wood and textile objects: Assessing gelled siderophores as novel green chelators. In *Gels in the Conservation of Art*; Archetype Books: London, UK, 2017.
33. Rapti, S.; Rivers, S.; Pournou, A. Removing iron corrosion products from museum artefacts: Investigating the effectiveness of innovative green chelators. In Proceedings of the International Conference "Science in Technology", SCinTE, Athens, Greece, 5–7 November 2015.
34. De Serrano, L.O. Biotechnology of siderophores in high-impact scientific fields. *Biomol. Concepts* **2017**, *8*, 169–178. [CrossRef]
35. Mahmoud, A.; Cézac, P.; Hoadley, A.F.A.; Contamine, F.; D'Hugues, P. A review of sulfide minerals microbially assisted leaching in stirred tank reactors. *Int. Biodeterior. Biodegrad.* **2017**, *119*, 118–146. [CrossRef]
36. Vaclavkova, S.; Jørgensen, C.J.; Jacobsen, O.S.; Aamand, J.; Elberling, B. The Importance of Microbial Iron Sulfide Oxidation for Nitrate Depletion in Anoxic Danish Sediments. *Aquat. Geochem.* **2014**, *20*, 419–435. [CrossRef]
37. Vaclavkova, S.; Schultz-Jensen, N.; Jacobsen, O.S.; Elberling, B.; Aamand, J. Nitrate-Controlled Anaerobic Oxidation of Pyrite by Thiobacillus Cultures. *Geomicrobiol. J.* **2015**, *32*, 412–419. [CrossRef]
38. Pelé, C.; Guilminot, E.; Labroche, S.; Lemoine, G.; Baron, G. Iron removal from waterlogged wood: Extraction by electrophoresis and chemical treatments. *Stud. Conserv.* **2015**, *60*, 155–171. [CrossRef]
39. Macchioni, N.; Capretti, C.; Sozzi, L.; Pizzo, B. Grading the decay of waterlogged archaeological wood according toanatomical characterisation. The case of the Fiavé site (N-E Italy). *Int. Biodeterior. Biodegrad.* **2013**, *84*, 54–64. [CrossRef]
40. Salmén, L. Wood cell wall structure and organisation in relation to mechanics. In *Plant Biomechanics*; Springer: Berlin/Hamburg, Germany, 2018; pp. 3–19.
41. Moosavinejad, S.M.; Madhoushi, M.; Vakili, M.; Rasouli, D. Evaluation of degradation in chemical compounds of wood in historical buildings using FT-IR and FT-Raman vibrational spectroscopy. *Maderas. Cienc. Y Tecnol.* **2019**, *21*, 381–392. [CrossRef]
42. Pandey, K.K.; Pitman, A.J. FTIR studies of the changes in wood chemistry following decay by brown-rot and white-rot fungi. *Int. Biodeterior. Biodegrad.* **2003**, *52*, 151–160. [CrossRef]
43. Pandey, K.K.; Theagar, K.S. Analysis of wood surfaces and ground wood by diffuse reflectance (DRIFT) and photoacoustic (PAS) Fourier transform infrared spectroscopic techniques. *Eur. J. Wood Wood Prod.* **1997**, *55*, 383–390. [CrossRef]
44. Dobrică, I.; Bugheanu, P.; Stănculescu, I.; Ponta, C. FT-IR spectral data of wood used in Romanian. *Analele Univ. Din Bucur.* **2008**, *1*, 33–37.
45. Macchioni, N.; Pecoraro, E.; Pizzo, B. The measurement of maximum water content (MWC) on waterlogged archaeological wood: A comparison between three different methodologies. *J. Cult. Herit.* **2018**, *30*, 51–56. [CrossRef]
46. Buchelt, B.; Wagenführ, A. Evaluation of colour differences on wood surfaces. *Eur. J. Wood Wood Prod.* **2012**, *70*, 389–391. [CrossRef]
47. Bouchard, M.; Smith, D.C. Catalogue of 45 reference Raman spectra of minerals concerning research in art history or archaeology, especially on corroded metals and coloured glass. *Spectrochim. Acta-Part A Mol. Biomol. Spectrosc.* **2003**, *59*, 2247–2266. [CrossRef] [PubMed]
48. Rémazeilles, C.; Tran, K.; Guilminot, E.; Conforto, E.; Refait, P. Study of Fe(II) sulphides in waterlogged archaeological wood. *Stud. Conserv.* **2013**, *58*, 297–307. [CrossRef]
49. El-Deen, S.S.; Hashem, A.M.; Abdel Ghany, A.E.; Indris, S.; Ehrenberg, H.; Mauger, A.; Julien, C.M. Anatase TiO_2 nanoparticles for lithium-ion batteries. *Ionics* **2018**, *24*, 2925–2934. [CrossRef]
50. Ostroumov, M. Raman and Infrared Reflection Spectroscopic Study of Mineralogical Composition of Iron-Manganese Nodules (Pacific and Indian Oceans). *Int. J. Exp. Spectrosc. Tech.* **2017**, *2*, 1–12. [CrossRef]
51. Ostroumov, M.; Gogichaishvili, A. Raman and Infrared reflection spectroscopic study of pre-Columbian Mesoamerican pottery. *Eur. J. Mineral.* **2013**, *25*, 895–905. [CrossRef]
52. Agarwal, U.P.; Ralph, S.A. FT-Raman Spectroscopy of Wood: Identifying Contributions of Lignin and Carbohydrate Polymers in the Spectrum of Black Spruce (*Picea mariana*). *Appl. Spectrosc.* **1997**, *51*, 1648–1655. [CrossRef]
53. Henrik-Klemens, Å.; Bengtsson, F.; Björdal, C.G. Raman spectroscopic investigation of iron-tannin precipitates in waterlogged archaeological oak. *Stud. Conserv.* **2022**, *67*, 237–247. [CrossRef]
54. Wiedenhoeft, A.C.; Miller, R.B. Structure and Function of Wood. In *Handbook of Wood Chemistry and Wood Composites*; CRC Press: Boca Raton, FL, USA, 2005.
55. Scalbert, A.; Monties, B.; Favre, J.-M. Polyphenols of *Quercus robur*: Adult tree and in vitro grown calli and shoots. *Phytochemistry* **1988**, *27*, 3483–3488. [CrossRef]
56. Grattan, D.W. Waterlogged wood. In *Conservation of Marine Archaeological Objects*; Elsevier: Amsterdam, The Netherlands, 1987; pp. 55–67.
57. Kreber, B. *Understanding Wood Discoloration Helps Maximize Wood Profits*; Western Dry Kiln Association: Corvallis, OR, USA, 1994.
58. Remazeilles, C.; Meunier, L.; Lévêque, F.; Plasson, N.; Conforto, E.; Crouzet, M.; Refait, P.; Caillat, L. Post-treatment Study of Iron/Sulfur-containing Compounds in the Wreck of Lyon Saint-Georges 4 (Second Century ACE). *Stud. Conserv.* **2020**, *65*, 28–36. [CrossRef]
59. Brunning, R.; Watson, J. *Waterlogged Wood: Guidelines on the Recording, Sampling, Conservation, and Curation of Waterlogged Wood*; CiNii: London, UK, 2010.

60. Perron, N.R.; Brumaghim, J.L. A review of the antioxidant mechanisms of polyphenol compounds related to iron binding. *Cell Biochem. Biophys.* **2009**, *53*, 75–100. [CrossRef]
61. Sandström, M.; Jalilehvand, F.; Damian, E.; Fors, Y.; Gelius, U.; Jones, M.; Salomé, M. Sulfur accumulation in the timbers of King Henry VIII's warship Mary Rose: A pathway in the sulfur cycle of conservation concern. *Proc. Natl. Acad. Sci. USA* **2005**, *102*, 14165–14170. [CrossRef] [PubMed]
62. Almkvist, G.; Norbakhsh, S.; Bjurhager, I.; Varmuza, K. Prediction of tensile strength in iron-contaminated archaeological wood by FT-IR spectroscopy-a study of degradation in recent oak and Vasa oak. *Holzforschung* **2016**, *70*, 855–865. [CrossRef]
63. Fors, Y.; Nilsson, T.; Risberg, E.D.; Sandström, M.; Torssander, P. Sulfur accumulation in pinewood (*Pinus sylvestris*) induced by bacteria in a simulated seabed environment: Implications for marine archaeological wood and fossil fuels. *Int. Biodeterior. Biodegrad.* **2008**, *62*, 336–347. [CrossRef]
64. Preston, J.; Smith, A.D.; Schofield, E.J.; Chadwick, A.V.; Jones, M.A.; Watts, J.E.M. The effects of Mary Rose conservation treatment on iron oxidation processes and microbial communities contributing to acid production in marine archaeological timbers. *PLoS ONE* **2014**, *9*, e84169. [CrossRef]
65. Beller, H.R.; Chain, P.S.G.; Letain, T.E.; Chakicherla, A.; Larimer, F.W.; Richardson, P.M.; Coleman, M.A.; Wood, A.P.; Kelly, D.P. The genome sequence of the obligately chemolithoautotrophic, facultatively anaerobic bacterium *Thiobacillus denitrificans*. *J. Bacteriol.* **2006**, *188*, 1473–1488. [CrossRef]
66. Schippers, A.; Jorgensen, B.B. Biogeochemistry of pyrite and iron sulfide oxidation in marine sediments. *Geochim. Cosmochim. Acta* **2002**, *66*, 85–92. [CrossRef]
67. Kelly, D.P.; Wood, A.P. Confirmation of *Thiobacillus denitrificans* as a species of the genus Thiobacillus, in the β-subclass of the Proteobacteria, with strain NCIMB 9548 as the type strain. *Int. J. Syst. Evol. Microbiol.* **2000**, *50*, 547–550. [CrossRef]
68. Torrentó, C.; Cama, J.; Urmeneta, J.; Otero, N.; Soler, A. Denitrification of groundwater with pyrite and *Thiobacillus denitrificans*. *Chem. Geol.* **2010**, *278*, 80–91. [CrossRef]
69. Berenguer, M.A.; Monachon, M.; Jacquet, C.; Junier, P.; Rémazeilles, C.; Schofield, E.J.; Joseph, E. Biological oxidation of sulfur compounds in artificially degraded wood. *Int. Biodeterior. Biodegrad.* **2018**, *141*, 62–70. [CrossRef]
70. Yan, R.; Kappler, A.; Muehe, E.M.; Knorr, K.-H.; Horn, M.A.; Poser, A.; Lohmayer, R.; Peiffer, S. Effect of reduced sulfur species on chemolithoautotrophic pyrite oxidation with nitrate. *Geomicrobiol. J.* **2019**, *36*, 19–29. [CrossRef]
71. MacLeod, I.D.; Kenna, C. Degradation of archaeological timbers by pyrite: Oxidation of iron and sulphur species. In Proceedings of the 4th ICOM-Group on Wet Organic Archaeological Materials Conference, Bremerhaven, Germany, 20–24 August 1990; pp. 133–142.
72. Passier, H.F.; Böttcher, M.E.; De Lange, G.J. Sulphur enrichment in organic matter of eastern Mediterranean sapropels: A study of sulphur isotope partitioning. *Aquat. Geochem.* **1999**, *5*, 99–118. [CrossRef]
73. Damste, J.S.S.; De Leeuw, J.W. Analysis, structure and geochemical significance of organically-bound sulphur in the geosphere: State of the art and future research. *Org. Geochem.* **1990**, *16*, 1077–1101. [CrossRef]
74. Aluri, E.R.; Reynaud, C.; Bardas, H.; Piva, E.; Cibin, G.; Mosselmans, J.F.W.; Chadwick, A.V.; Schofield, E.J. The Formation of Chemical Degraders during the Conservation of a Wooden Tudor Shipwreck. *Chempluschem* **2020**, *85*, 1632–1638. [CrossRef] [PubMed]
75. Mortensen, M.N.; Chaumat, G.; Gambineri, F.; Kutzke, H.; Łucejko, J.J.; Modugno, C.M.A.; Modugno, F.; Tamburini, D.; Taube, M. Climatically induced degradation processes in conserved archaeological wood studied by time-lapse photography. *Stud. Conserv.* **2019**, *64*, 115–123. [CrossRef]
76. Gargano, E.M.; Mangiatordi, G.F.; Weber, I.; Goebel, C.; Alberga, D.; Nicolotti, O.; Ruess, W.; Wierlacher, S. Persulfate Reaction in a Hair-Bleaching Formula: Unveiling the Unconventional Reactivity of 1, 13-Diamino-4, 7, 10-Trioxatridecane. *ChemistryOpen* **2018**, *7*, 319–322. [CrossRef]
77. Anipsitakis, G.P.; Dionysiou, D.D. Radical generation by the interaction of transition metals with common oxidants. *Environ. Sci. Technol.* **2004**, *38*, 3705–3712. [CrossRef]
78. Norvell, W.A. Equilibria of metal chelates in soil solution. In *Micronutrients in Agriculture*; Soil Science Association of America: Madison, WI, USA, 1972.
79. Farkas, E.; Enyedy, É.A.; Csóka, H. A comparison between the chelating properties of some dihydroxamic acids, desferrioxamine B and acetohydroxamic acid. *Polyhedron* **1999**, *18*, 2391–2398. [CrossRef]
80. Sullivan, S.; Mackay, R. *Archaeological Sites: Conservation and Management*; Getty Publications: Los Angeles, CA, USA, 2012; Volume 5.
81. Matthiesen, H.; Eriksen, A.M.H.; Hollesen, J.; Collins, M. Bone degradation at five Arctic archaeological sites: Quantifying the importance of burial environment and bone characteristics. *J. Archaeol. Sci.* **2021**, *125*, 105296. [CrossRef]
82. Lucejko, J.J.; Tamburini, D.; Zborowska, M.; Babiński, L.; Modugno, F.; Colombini, M.P. Oak wood degradation processes induced by the burial environment in the archaeological site of Biskupin (Poland). *Herit. Sci.* **2020**, *8*, 44. [CrossRef]
83. Babiński, L.; Zborowska, M.; Gajewska, J.; Waliszewska, B.; Prądzyński, W. Decomposition of the contemporary oak wood (*Quercus* sp.) in conditions of the wet archaeological site in Biskupin. *Folia For. Pol.* **2006**, *37*, 9–21.

84. Tamburini, D.; Łucejko, J.J.; Zborowska, M.; Modugno, F.; Cantisani, E.; Mamoňová, M.; Colombini, M.P. The short-term degradation of cellulosic pulp in lake water and peat soil: A multi-analytical study from the micro to the molecular level. *Int. Biodeterior. Biodegrad.* **2017**, *116*, 243–259. [CrossRef]
85. Monachon, M.; Albelda-Berenguer, M.; Pelé, C.; Cornet, E.; Guilminot, E.; Rémazeilles, C.; Joseph, E. Characterization of model samples simulating degradation processes induced by iron and sulfur species on waterlogged wood. *Microchem. J.* **2020**, *155*, 104756. [CrossRef]